Geomechanics for Energy and the Environment 39 (2024) 100577

Contents lists available at ScienceDirect

Geomechanics for Energy and the Environment

journal homepage: www.elsevier.com/locate/gete

Value of abstraction in performance assessment – When is a higher level of detail necessary?

Tanja Frank [a], Dirk-Alexander Becker [a,*], Steven Benbow [c], Alexander Bond [c], Richard Jayne [b], Tara LaForce [b], Jens Wolf [a]

[a] Gesellschaft für Anlagen- und Reaktorsicherheit (GRS) gGmbH, Braunschweig, Germany
[b] Sandia National Laboratories (SNL), Albuquerque, United States
[c] Quintessa, Warrington, United Kingdom

ARTICLE INFO

Editors-in-Chief: Professor Lyesse Laloui and Professor Tomasz Hueckel

Keywords:
Performance assessment
Domal salt
Model uncertainty
Radioactive waste disposal
Safety assessment
Radionuclide transport simulation

ABSTRACT

In this study, different approaches in performance assessment (PA) of the long-term safety of a repository for radioactive waste were examined. This investigation was carried out as part of the DECOVALEX-2023 project, an international collaborative effort for research and model comparison. One specific task of the DECOVALEX-2023 project was the Salt Performance Assessment Modelling task (Salt PA), which aimed at comparing various models and methods employed in the performance assessment of deep geological repositories in salt. In the context of the Salt PA task, three distinct teams from SNL (United States), Quintessa Ltd (United Kingdom), and GRS (Germany) examined the consequences of employing different levels of abstractions when modelling the repository's geometry and implementing various features and processes, using the example of a simple hypothetical repository structure in domal salt. Each team applied their own tools: PFLOTRAN (SNL), QPAC (Quintessa) and LOPOS (GRS). These differ essentially regarding numerical concept and degree of detail in the representation of the underlying physical processes. The discussion focused on when simplifications can be appropriately applied and what consequences result from them. Furthermore, it was explored when and if a higher level of fidelity in geometry or physical processes is required.

1. Introduction

The assessment of the long-term safety of a repository for radioactive waste involves a dual challenge: it must adhere to legal regulations, which require statements that are valid over very long timeframes, and, at the same time should take into account the ever-evolving state of science and technology. This challenge requires that simulators, on the one hand, represent the intricate processes within a repository system with sufficient accuracy and, on the other hand, provide a numerically efficient approach to produce reliable safety statements for the extended time frames mandated by regulations and thus support decision making. Therefore, the principle that guides performance assessment (PA) is parsimony; to be as simple as possible while retaining the necessary complexity. PA serves as an iterative tool during site selection and characterization, increasing confidence in the system and aiding in the understanding of its possible evolution.

In the context of DECOVALEX-2023, the Salt Performance Assessment Modelling Task carried out a comparative evaluation of models and methods used in the assessment of deep geological repositories. This project involved the development of a PA scenario for a repository in domal salt (LaForce et al.[1]). Teams from five different organisations (BASE, Quintessa, SNL, COVRA, GRS) participated in this task, aimed at comparing and discussing their various perspectives and approaches. Each team employed a different software tool and devised a modelling strategy to tackle this common challenge. Teams created a conceptual model and reached a consensus on defining parameters that encompass features, events, and processes influencing performance. The primary objective of this effort was to increase confidence in the models, methods, and software used for deep geologic repository performance assessment. It also sought to identify areas for additional research and development to enhance PA methodologies. To accommodate the capabilities of the software, ensure a simulation time of 100,000 years, and test proven approaches from the past, several simplifications were made. Teams explored diverse modelling approaches to evaluate the consequences of these simplifications, including variations in the level of detail representing the simulation grid (e.g., shaft and drift

* Corresponding author.
E-mail address: dirk-alexander.becker@grs.de (D.-A. Becker).

https://doi.org/10.1016/j.gete.2024.100577
Received 6 February 2024; Received in revised form 20 June 2024; Accepted 16 July 2024
Available online 21 July 2024

representation, and inclusion of the host rock) and in the implementation of features and processes like salt compaction. The specific exercise described here was carried out by three of these teams (SNL, Quintessa, GRS). The key question was where simplifications are necessary or sensible and where they are also permissible.

2. Methods

2.1. Model setup

Multiple PAs, including KOSINA, RESUS, and the Preliminary Safety Analysis for Gorleben (Bollingerfehr et al.[2,4], Bertrams et al.[3]) have conclusively demonstrated that there are no significant radiological consequences via liquid-phase transport for 1,000,000 years in the case of the expected evolution of a repository system in a salt formations because of salt's very low permeability and moisture content. Therefore, the current focus is on an alternative scenario, where shaft seals fail 1000 years after repository closure. This results in the inflow of brine from an overlying aquifer down the shafts and into the repository. The case involves a repository in a salt dome for spent nuclear fuel (SNF) and vitrified high-level waste (HLW). Transport simulations focus on a limited set of radionuclides: I-129 (a single long-lived fission product), Tc-99, and a single transuranic decay chain (U-238 → U-234 → Th-230 → Ra-226). The inventory of SNF comprises pressurized water reactor (PWR) fuel assemblies packaged in 500 POLLUX-10 containers, each holding 10 assemblies. The case also covers vitrified high-level waste (HLW) resulting from SNF reprocessing, mirroring COGEMA's Dutch fuel cycle waste characteristics (Meleshyn and Noseck[5]). There are 500 HLW canisters, each with 400 kg of waste, following the same radionuclide decay chain as SNF, except for I-129, which is not present. An initial release fraction (IRF) of 10 % is applied to I-129, and the IRF is zero for all radionuclides in the U-238 decay chain. Details of the modelled inventory are given in Table 1.

The POLLUX-10 containers are assumed to confine waste for 500 years, after which they offer no further containment. Dissolution of the fuel matrix (UO_2) occurs at a fractional rate of 10^{-7} per year. The scenario excludes any protective influence from the steel canister enclosing the vitrified glass. The vitrified glass dissolves at a constant rate of $3.8727 \bullet 10^{-7}$ per year. Tracer 1 and Tracer 2 in the SNF simulate the behaviour of I-129, Tracer 1 representing the IRF and Tracer 2 the rest of the I-129 inventory. Tracer 3 is released from the vitrified glass in the HLW, representing the characteristics of Tc-99 (LaForce et al.[1]).

The repository is located 850 m below the surface and is designed to be symmetric. Fluid pressure in the geosphere is defined as hydrostatic and a temperature of 38 °C is assumed. Access is provided by two 850 m tall shafts with 7 m by 7 m cross sections, designed to prevent water ingress and radionuclide transport. An assumption of identical boundary conditions on the two access shafts allows only half of the system to be modelled due to symmetry. Inside the repository there are three sets of 25 emplacement drifts (Fig. 1). All drifts and access tunnels have dimensions of 7 m width and 4 m height. The infrastructure area, with a total volume of 240,000 m^3, is filled with gravel allowing for fluid or gas accumulation during the post-closure phase. Emplacement drifts and access tunnels are filled with compacting run-of-mine salt. Material properties are detailed in Table 2. The layered shaft seal design and the simplified homogeneous shaft design are shown in Fig. 1. The layered design contains segments designed to seal and segments designed to act as reservoirs. Initial material properties in the layered shaft are given in Table 3. After shaft seal failure, the permeability of each layer in the layered shaft is assumed to increase by two orders of magnitude. The harmonic average of the layers weighted by the thickness of each layer is calculated for the bulk permeability of the simplified shaft. The arithmetic average of the porosities, weighted by the thickness of each layer is used for the bulk porosity of the simplified shaft, to give a total pore volume consistent with the layered shaft model. Thus, the permeability of the simplified shaft changes from $8.6232 \bullet 10^{-18}$ m^2 to $2.0606 \bullet 10^{-16}$ m^2 after 1000 years and the porosity is always 0.24. The mined repository is assumed to have a 20 % initial liquid saturation with a gas phase (if present) at atmospheric pressure across all regions. This is a relatively high value and was chosen to address numerical challenges in simulating lower saturations using the specified relative permeability models, which are listed in Table 4. The shaft has an initial liquid saturation of 35 %.

Table 1
Inventory of one POLLUX-10 container and HLW canister, and their respective nuclide solubility.

Isotope	Inventory per POLLUX-10 container [g] (SNF)	Inventory [g/canister] HLW	Solubility [mol/kg]
U-234	$2.22 \bullet 10^3$	2.06	$1.12 \cdot 10^{-7}$
U-238	$3.96 \bullet 10^6$	$4.45 \bullet 10^3$	$1.12 \cdot 10^{-7}$
Th-230	$4.52 \cdot 10^{-1}$	$2.25 \cdot 10^{-4}$	$4 \cdot 10^{-3}$
Ra-226	$1.74 \cdot 10^{-4}$	$2.82 \cdot 10^{-9}$	10^{-3}
I-129	$1.36 \bullet 10^3$	-	Unlimited
Tc-99	-	$1.99 \bullet 10^3$	Unlimited
Tracer-1	136.2	-	Unlimited
Tracer-2	1226	-	Unlimited
Tracer-3	-	1990	Unlimited

2.2. Conceptual approach

Different software tools were used by different teams to model the PA Task in domal salt. A comprehensive overview of the modelling tools and approaches, along with the features and processes, is presented in Table 5. For an in-depth understanding of PFLOTRAN, please refer to Hammond et al.[10]. Furthermore, for a detailed insight into QPAC refer to Quintessa[11], and for an extensive description of LOPOS, consult Hirsekorn et al.[12].

QPAC is a finite volume code, with the capability to flexibly specify equations governing the evolution of variables on the interfaces between finite volumes, and at the volume centroid via the input language. Predefined "modules" of collections of physics (e. g., thermal, multi-phase flow) are available and have been tested to support rapid development of new models. The computations are conducted monolithically, where all equations are solved simultaneously, employing a fully implicit time-stepping approach. This method facilitates the complete integration of all simulated processes, encompassing creep closure. The model implementation and gridded model are depicted in Fig. 2.

PFLOTRAN (Hammond et al.[10]) is an open source, state-of-the-art massively parallel subsurface flow and reactive transport code. PFLOTRAN solves a system of generally nonlinear partial differential equations describing multiphase, multicomponent and multiscale reactive flow and transport in porous materials. The code is designed to run on massively parallel computing architectures as well as workstations and laptops. PFLOTRAN is developed by Sandia National Laboratory (SNL) for nuclear waste disposal applications and utilizes the Finite Volume method. It is possible to simulate on Voronoi or Cartesian meshes in 3D. For the current task, salt compaction from crushed salt to the properties of intact salt is depicted as a permeability decrease by seven orders of magnitude, neglecting the reduction of pore volume, as this would cause mass conservation issues. The model grid developed for this task is shown in Fig. 3 (left).

GRS developed the LOPOS (Loop structures in repositories) integrated safety assessment code for modelling one-dimensional, single-phase transport within a nuclear waste repository in salt (Hirsekorn et al.[12]). LOPOS is part of the RepoTREND code package (Reiche[13]). This code simulates brine inflow, its path through the mine to the waste, radionuclide release, and subsequent movement within the mine, ultimately reaching the shaft's top. It computes fluid pressure, brine flow, and radionuclide transport using a nonlinear balance equation, with the

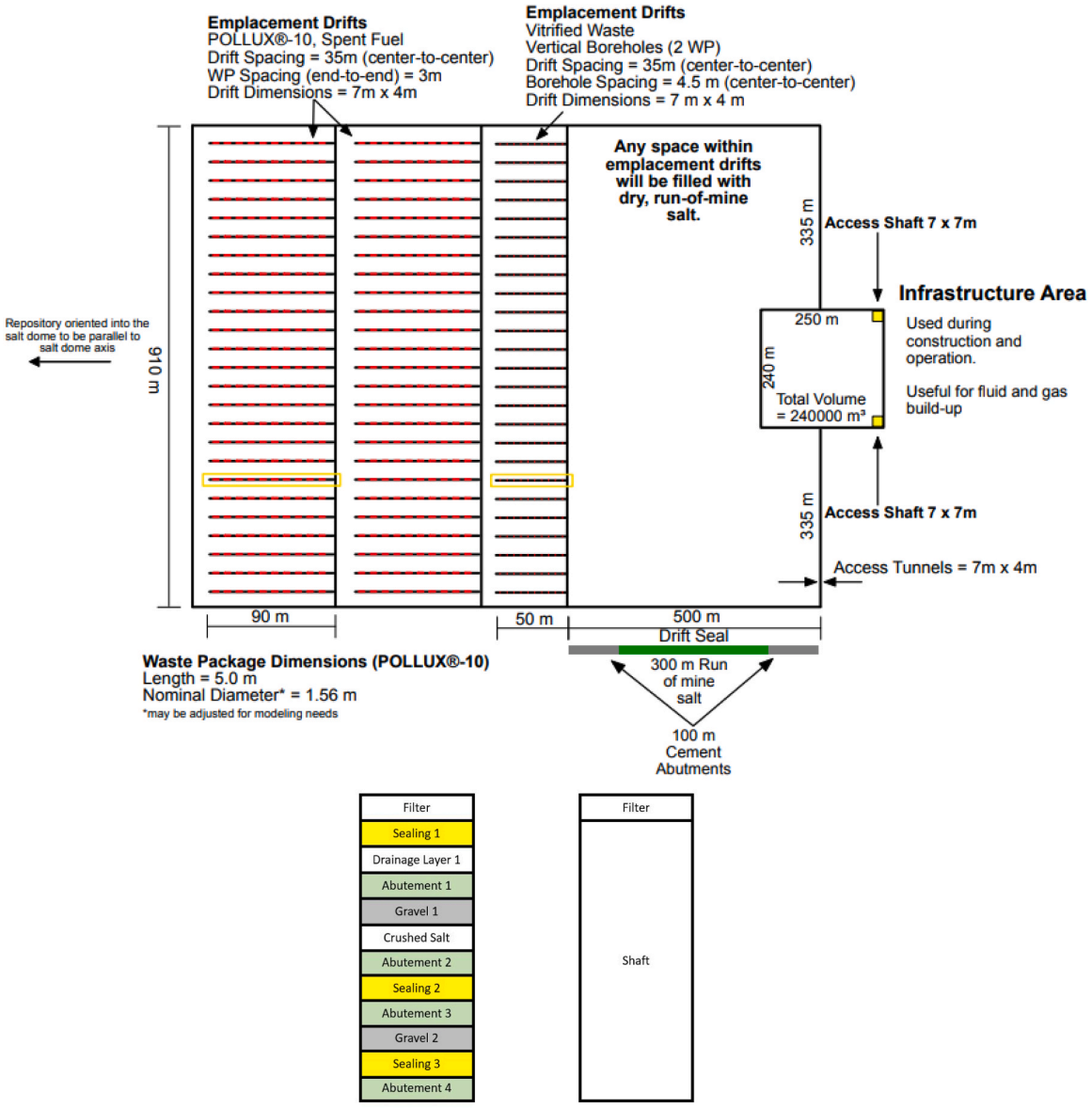

Fig. 1. Spatial dimensions of the model geometry (top) and comparison of the layered shaft design and the simplified homogeneous shaft design (bottom) (LaForce et al.[1]).

Table 2
Material properties for the shaft, drifts (crushed salt), the infrastructure area (gravel), and the sealing (abutment).

	Intrinsic permeability [m^2]	Porosity [-]	Effective diffusion coefficient [m^2/s]
Crushed Salt[a]	$8.35 \cdot 10^{-15}$	0.1	$2.3 \cdot 10^{-11}$
Sorel cement (drift seals)[b]	$5 \cdot 10^{-17}$	0.13	$3.9 \cdot 10^{-11}$
Gravel (infrastructure area)[b]	10^{-14}	0.3	$2.1 \cdot 10^{-10}$
Homogeneous shaft seal before failure[c]	$8.6232 \cdot 10^{-18}$	0.24	$1.3 \cdot 10^{-10}$
Homogeneous shaft seal after failure[c]	$2.0606 \cdot 10^{-16}$	0.24	$1.3 \cdot 10^{-10}$

[a] Estimated after 1000 years of reconsolidation from results by Blanco-Martin et al.[6].
[b] Rübel et al.[7].
[c] Data from Rübel et al.[7]. Volume weighted average porosity estimated from shaft seal design.

Table 3
Material properties for the layered shaft model prior to seal failure. After shaft failure the permeability of each layer increases by two orders of magnitude (LaForce et al.[1]).

	Intrinsic vertical permeability [m^2]	Porosity [-]
Filter/Inlet	10^{-12}	0.3
Sealing Element 1	10^{-17}	0.27
Drainage Layer 1	10^{-12}	0.25
Abutment 1	10^{-12}	0.1
Gravel 1	10^{-09}	0.23
Crushed Salt	$1.3 \cdot 10^{-12}$	0.1
Abutment 2	$2 \cdot 10^{-15}$	0.1
Sealing Element 2	$7 \cdot 10^{-19}$	0.1
Abutment 3	$2 \cdot 10^{-15}$	0.1
Gravel 2	10^{-09}	0.38
Sealing Element 3	$5 \cdot 10^{-17}$	0.16
Abutment 4	$5 \cdot 10^{-17}$	0.16

Table 4
Relative permeability parameters.

	Intact salt[a]	Crushed salt[a]	Shaft seal[a]	Concrete[b]	Gravel[c]
Relative Permeability Function	Corey	Corey	Corey	Mualem-VG	VG
Residual Liquid Sat	0.10	0.03	0.03	0.20	0.19
Residual Gas Sat	0.00	0.00	0.00	0.10	0.00
Van Genuchten's λ [-]	0.60	0.60	0.60	0.56	0.675
Van Genuchten's P_0 [MPa]	5.70	1.60	1.60	7.70	1.60
Van Genuchten's S_{lr}	0.01	0.02	0.02	0.00	0.00

[a] Blanco-Martin et al.[6].
[b] Ecay et al.[8].
[c] Osselin et al.[9].

Table 5
Overview of modelling tools, techniques, features, and processes.

Team	SNL	Quintessa	GRS
Modelling tools	PFLOTRAN	QPAC	RepoTREND (LOPOS)
Modelling approach	3D Cartesian Mesh with ½ symmetry	1D and 2D models linked together	Segmented model of 1D compartments, connected in three dimensions
Numerical method	Finite Volume	Finite Volume	Finite Difference
Dimensions	3D	3D	1D
Includes hostrock	Yes	No	No
Includes overburden	Yes	No	No
Full repository Continuous or compartment model	No, symmetric Continuous	No, symmetric Continuous	No, symmetric Compartment
Flow model	Richards equation	Richards equation (Darcy and multi-phase flow in variants)	Darcy equation (Richards equation in variants)
Compaction setup	Porosity and Permeability decrease at different time steps	Re-implementation of LOPOS model	Fully coupled implementation

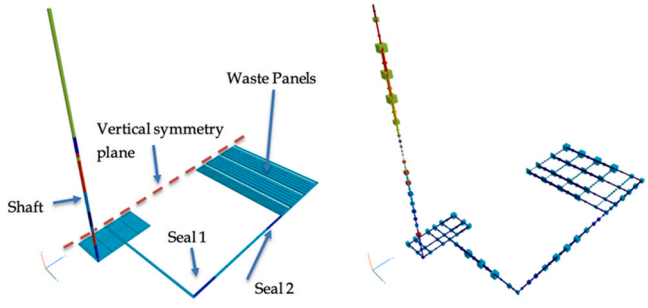

Fig. 2. The Quintessa model grid in QPAC, with intrinsic permeability colour-coded on a logarithmic scale, showing a 1D (left) and volumetric representation (right) with compartment volumes indicating cell sizes, including the layered shaft infill.

continuity equation as the foundation. Flow is assumed to follow Darcy's law and radionuclide transport employs the finite differences method with variable time stepping, encompassing advection, dispersion, and diffusion. Time discretization is managed according to the equation solver's stability criteria. The model domain for the current task is illustrated in Fig. 3 (right).

2.3. Governing processes

There are various ways to simplify PA modelling, both in terms of geometry and the consideration and representation of different processes. This section outlines the features and processes investigated within the scope of the DECOVALEX Salt PA Task. It includes a discussion of the potential significance of these processes for PA and elaborates on their modelling, abstraction, and simplification.

2.3.1. Geometry variations

With respect to the geometry of the system, there are various possibilities of simplifications. One option is to model each of the 25 emplacement chambers and boreholes individually or to group them together. This was also explored by GRS. Quintessa examined the impact of the selected discretization within the drifts and tunnels. Another geometric variation, which will not be further discussed here is the use of Voronoi mesh and Cartesian mesh in PFLOTRAN. Another geometric simplification is the representation of the shaft, which will be addressed in the next section.

2.3.2. Shaft variations

The description provided for the shaft refers to the repository concept developed as part of the Preliminary Safety Analysis for Gorleben (Rübel et al.[7]). The shaft seals are composed of three short-term sealing components, one long-term sealing component (crushed salt), and several additional components such as abutments and reservoirs. The placement of each component is determined by the geological structures of the Gorleben Bank. Short-term sealing materials are selected based on criteria, including, permeability similar to that of the host rock, stability against chemical and biological erosion, stability in the presence of brines, and long-term durability. In Rübel et al.[7], the short-term sealing materials are chosen as follows: The first sealing component is constructed from bentonite, possessing material properties similar to the salt clay near the top of the salt rock. It exhibits a high cation exchange capacity, and its swelling pressure enables the closure of the excavation-damaged zone (EDZ) at shallow depths with minimal rock pressure. This makes it suitable for use in the upper short-term sealing component. The second sealing component is comprised of salt concrete. Salt concrete remains stable when exposed to the expected brines in this location, providing an alternative to bentonite. Directly above the disposal level, a third sealing component consists of sorel concrete. Sorel concrete is composed of magnesium oxide and crushed salt. These three sealing components are designed as short-term seals for several hundred years, intended to maintain their functionality until the backfill compaction in the mine galleries is completed. Additionally, there is a long-term sealing component in the shaft made of crushed salt, situated between the two concrete sealing elements. Over time, this salt layer compacts and attains a permeability and porosity that equals that of the host rock (Rübel et al.[7]).

Within this study the behaviour of the layered shaft and the simplified homogeneous shaft is compared. LOPOS and QPAC have performed these calculations. A discussion is conducted to determine if the consolidation of individual shaft elements into one modelled element is permissible and if this leads to any limitations.

2.3.3. Flow assumptions

Taking into account two-phase flow processes is important in performance assessment. However, determining the parameters is challenging, and even more difficult is predicting their changes over time. The extent to which two-phase processes play a role and their relevance depends on parameterization. For example, the results of a project for the final repository in Morsleben strongly depended on the selected

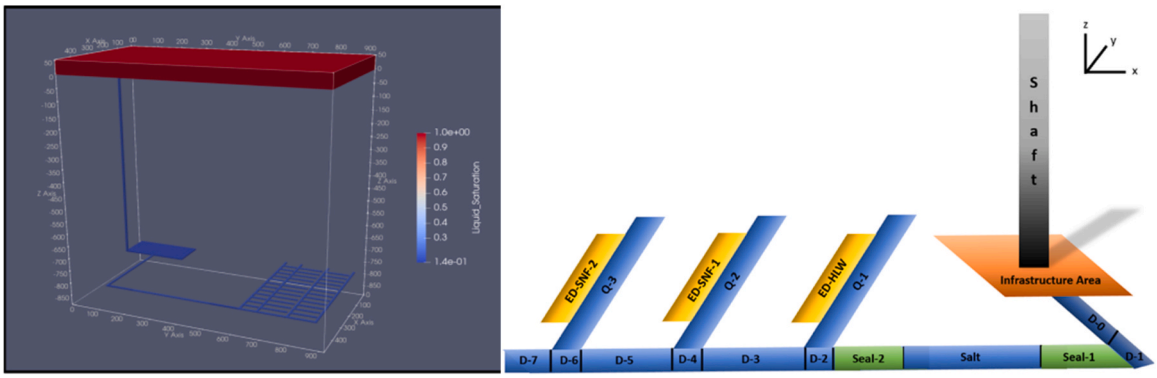

Fig. 3. PFLOTRAN model domain (left) including the repository, shaft, and overlying aquifer with initial fluid saturation and LOPOS layout (right) featuring distinct colours for various materials.

input data (Frieling and Kock[14]), and the results had limited applicability. For the preliminary analysis for Gorleben (Larue et al.[15]), the two phase parametrization was chosen to avoid numerical issues. Further research is needed to reliably quantify these parameters. For the present case, the constitutive models of Corey, Van Genuchten (VG), and Mualem-VG were used. A description of these can be found in Hammond et al.[10] and Bond et al.[16].

However, there are other ways to model flow in a porous medium (for PA) beside two-phase flow. In this context, we will compare the uses of single-phase Darcy flow, the Richards equation, and multiphase flow.

LOPOS exclusively employs Darcy flow in fully saturated model compartments. In partially saturated compartments, no transport of contaminants is calculated, and fluid movement is due to pressure differences. The saturation process in LOPOS is monitored by a simple fluid and void volume balance. QPAC can be used in any of the three flow approaches. For this study, PFLOTRAN utilizes the Richards equation, and also implementing single-phase Darcy flow where the domain is fully saturated. Below is a brief description of the differences. We refer to the literature about the respective codes. Darcy flow describes the movement of a single-phase fluid (typically water or brine) through a fully saturated porous medium driven by pressure gradient. It is based on Darcy's law, which defines the velocity of liquid flow through porous media as a function of factors like permeability and hydraulic gradient.

The Richards equation describes the transport of fluid movement in porous media with varying saturation. It extends Darcy's law to account for the influence of a second phase (air) without modelling this phase explicitly. Instead, the gas phase is assumed to be infinitely mobile, and so calculation of the gas pressure gradient is not required. Multiphase flow refers to the movement of multiple fluid phases, e.g., water and air, in a porous or fractured medium. This approach considers the interactions between different fluid phases and can describe the transport of both liquids and gases in complex systems. The impact of the flow models on radionuclide transport is investigated by comparing liquid-phase radionuclide transport and relative liquid saturation.

2.3.4. Compaction models

Salt rock is plastically deformable under applied differential stress, allowing it to creep into existing cavities. This process is referred to as salt rock convergence. The convergence process leads to a reduction of the remaining void spaces and an increase in the brine and gas flow resistance. The reduction of remaining void spaces leads to displacement of pore fluids which can increase the amount of brine that comes into direct contact with the emplaced waste. In contrast, the increase of flow resistance hinders the inflow of brine into storage locations. If the brine has reached the storage locations and radionuclides have been released from the waste packages before the pathways are sealed by convergence, the reduction in cavity volume results in the squeezing out of contaminated brine. In this case, advection is the primary driving mechanism for radionuclide release while convergence is ongoing. The convergence process can, on one hand, act as a sealing effect, isolating the repository inventory from the biosphere, and, on the other hand, facilitate radionuclide release. The actual behaviour depends on the specific scenario, location, and design of the repository and, therefore, each case must be individually examined. This is why this process holds significant importance in salt modelling.

The convergence process varies with factors such as convergence rate, moisture, and temperature. We employed Gorleben data for drift convergence modelling (Bertrams et al.[3]) as computed by LOPOS, which uses a salt creep model based on equations from Hirsekorn et al.[12] and Noseck et al.[17], as presented below. Quintessa incorporated the LOPOS salt creep model in QPAC. SNL is applying a stepwise permeability adjustment after 1000 years. When the shaft failure occurs, it is assumed in PFLOTRAN that drift convergence is almost complete, and all crushed salt within the repository takes on the permeability characteristics of intact salt. However, porosity remains constant over time to ensure the conservation of mass.

The change of pore volume (V_P) in salt is determined by LOPOS/QPAC over time through the following equations:

$$\frac{d}{dt}V(t) = -K(t) \bullet V(t) \quad (1)$$

$$K(t) = L \quad K_{ref} \bullet f_R \bullet f_P \bullet f_F \bullet f_T \quad (2)$$

where:

- $V(t)$ is volume of a compartment at time t [m^3],
- $K(t)$ is the convergence rate at time t [1/y],
- L is the factor for local properties of the surrounding salt [-],
- K_{ref} is the reference convergence rate [1/y],
- f_R is the moisture creep enhancement function [-],
- f_P is the fluid pressure function [-],
- f_F is the backfill support function [-],
- f_T is the temperature function [-].

f_P governs the convergence rate's reliance on liquid pressure in the pore space. Consequently, the convergence rate depends on the difference between rock pressure and liquid pressure at a specific depth. f_F describes the dependence of the convergence rate on the porosity of the backfill material that might be present in the cavity. With decreasing porosity, the backfill gets stiffer and hinders further convergence. Lower porosity corresponds to increased backfill support. In LOPOS, f_F is calculated using an approach described in Noseck et al.[12]. f_T considers the ability of elevated temperatures to amplify the salt's creep rate, leading to quicker cavity convergence. In the current isothermal scenario, f_T is not used, and thus, $f_T = 1$. In cases where liquid infiltrates the surrounding rock and alters its mechanical properties, the creep rate in a

mine can increase. This increased convergence rate is addressed by the function fR. The reduction of the compartment volume V and pore volume VP is calculated based on the equations established by Storck et al.[18]:

$$V(t+\Delta t) = V(t)(1-K(t)\Delta t)$$

$$V_P(t+\Delta t) = V_P(t) - V(t)K(t)\Delta t$$

and porosity is adjusted to

$$\Phi(t+\Delta t) = \frac{V_P(t+\Delta t)}{V(t+\Delta t)}.$$

2.3.5. Initial conditions

The initial conditions have a large impact on the results of the simulation. It is important to carefully select the input data as they have a significant impact on the quality and reliability of the model's outcomes. The determination of initial conditions for repositories are nevertheless site-specific and challenging due to uncertainties and variability in initial properties of the system. In particular, the disturbance to the host rock due to construction activities (e.g., the extent of the EDZ and its properties) is difficult to quantify. Additionally, the initial saturation is difficult to assign since the backfill is likely to be emplaced sequentially and so even if emplaced with an identical saturation, the saturation field in the backfill at the initial time assumed in the model is not likely to be uniform throughout the repository. However, for simplicity a uniform initial saturation is usually assumed. A high initial saturation can significantly influence the behaviour of the repository, as it can have effects on hydrological and mechanical stability. We discussed the consequences of the (high) initial saturation of 20 % in the repository and 35 % in the shaft. Additionally, the choice of parameterization for salt compaction is discussed.

2.3.6. Geosphere inflow

Intact rock salt forms an impermeable barrier to both gas and brine. Given the extremely low permeability of intact salt, around 10^{-22} m^2, it is assumed that the hydraulic conductivity is so minimal that no liquid can infiltrate the repository through the intact salt. For this reason, the access drifts are considered to be the primary pathways for radionuclide transport. This assumption forms the basis for various calculations (Larue et al.[15], Bertrams et al.[3], Becker et al.[19]). Furthermore, salt drifts will be surrounded by an excavation damage zone (EDZ), which has a higher permeability than the intact rock, which could lead to brine inflow to the drifts. To assess the potential impact of liquid ingress from EDZ or geosphere, Quintessa conducted calculations both with and without such ingress using QPAC. In contrast, SNL exclusively conducted calculations considering liquid ingress from the geosphere using PFLOTRAN since that is common in their approach to PAs.

As per the findings from Task E Brine Availability Task (BATS) in DECOVALEX-2023, an illustrative brine inflow rate of 1 g/day/m tunnel length was assigned in the QPAC variation to all tunnels at the repository level.

3. Results and discussion

In this chapter, the differences resulting from varying levels of detail are discussed. It is examined what benefits or drawbacks arise from increased detail and when do dissimilar models yield similar results?

3.1. Geometry variations

Calculations were carried out with LOPOS to investigate whether it is permissible to consolidate the 25 adjacent emplacement drifts and boreholes into a single entity. Regarding the radionuclide release from these drifts and boreholes and their saturation process, minimal differences were observed, extending only to the third valid decimal place. This is considered negligible. Quintessa discovered through variations that including a vertical discretisation in the drifts and tunnels did not significantly affect the results. From these investigations, it was concluded that it is permissible to combine the 25 adjacent emplacement chambers and boreholes and neglect vertical discretisation in the drifts and tunnels, as the consequences are minimal, while significantly reducing computational time. A short computation time is important because sensitivity analyses are part of the performance assessment, necessitating a multitude of calculations.

3.2. Shaft variations

Calculations were conducted with QPAC and LOPOS to examine the consequences resulting from simplifying the layered shaft design to a homogeneous one. It should be repeated in this context that unlike QPAC, LOPOS is not a two-phase code and actually does not calculate fluid saturation but the ratio of fluid volume and accessible pore volume in each compartment, resulting in one single value per shaft layer, based on Darcy flow with simplified assumptions about fluid pressure and flow resistance. Therefore, the results of LOPOS and QPAC represent different abstractions and should be compared with care.

The most striking difference between QPAC and LOPOS is the time needed for reaching full saturation of the shaft. Both codes start with an initial saturation of 35 %, but while in QPAC 100 % are reached after a little more than 5000 years, this takes more than three times as long in

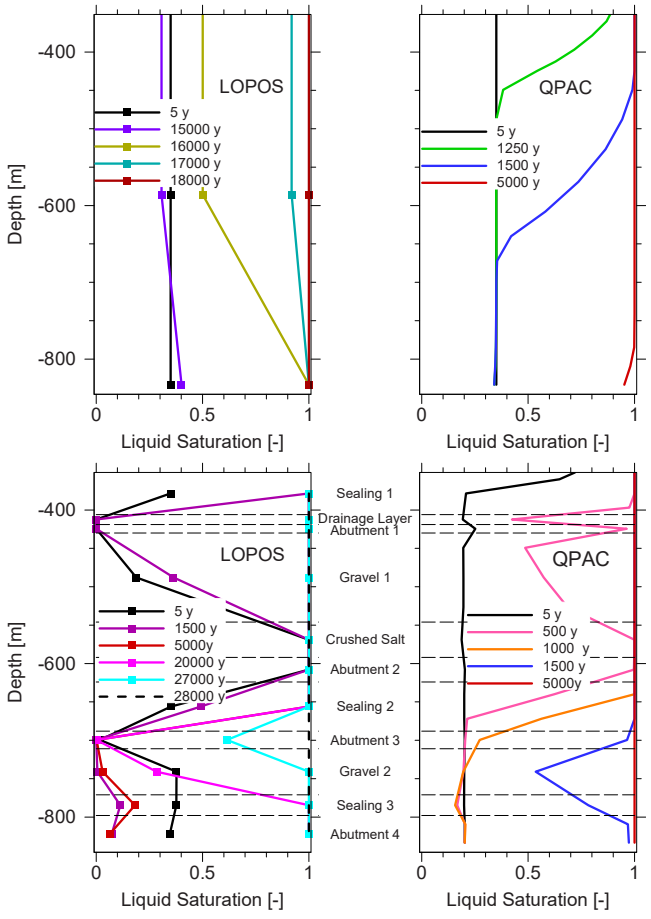

Fig. 4. Saturation of the homogeneous shaft (top) and the layered shaft (bottom), calculated by LOPOS and QPAC. Curves with the same colour represent the same time. The dashed lines separate the shaft layers (see Fig. 1). Note that for LOPOS, only one value per shaft segment is valid, formally located in the middle of the layer and indicated by square symbols. The lines are for better visibility and have no physical meaning.

LOPOS (see Fig. 4, top). Obviously, two-phase effects play a dominating role in the re-saturation process.

When comparing the layered shaft with the homogeneous shaft, some differences are observed. LOPOS calculates that in the homogeneous case, the shaft becomes completely saturated after 17,400 years, whereas the layered shaft takes 28,000 years to reach full saturation. This difference is not negligible since it covers 10 % of the assessment period, but the homogeneous case is considered to be conservative since it leads to a more rapid saturation and consequently to earlier and higher radionuclide release. Additionally, what becomes apparent in the layered design is the effectiveness of the seals. They exhibit low hydraulic conductivity; the liquid volume in the LOPOS compartments initially flows into the underlying compartments, and less liquid intrudes from above, causing the compartments to desaturate initially (Fig. 4, bottom left). The Drainage Layer, Abutment 1 and Gravel 1 desaturate first because Sealing 1 holds the liquid back, causing the liquid to accumulate in the compartments Abutment 2 and Crushed Salt. In these two compartments, the liquid accumulates due to the low-permeability layer Sealing 2, which is also responsible for the desaturation of Abutment 3, Gravel 2, Sealing 3, and Abutment 4. Note that Sealing 3 has higher permeability than the two sealing elements above it.

In contrast to LOPOS, QPAC calculates a faster saturation phase than for the homogeneous shaft (Fig. 4, bottom right): While in the homogeneous case full saturation is reached after 6000 years, it takes only 3000 years in the heterogeneous case. Relevant desaturation does not occur with QPAC. As in the homogeneous case, the total re-saturation process is significantly faster than with LOPOS. The most relevant contrast between QPAC and LOPOS with both shaft models lies in the re-saturation of the infrastructure area (Fig. 5), highlighting that re-saturation beyond the seals is predominantly driven by compaction rather than shaft inflow. For the LOPOS calculations, complete saturation of the infrastructure area is reached at nearly the same time in both cases, even though the saturation process for the case with the layered shaft progresses a bit more slowly. This reflects the delayed saturation of the layered shaft. The difference between LOPOS and QPAC appears to reflect the different approaches to dealing with water retention in the shaft volumes.

The assumption of a homogeneous shaft leads, in case of QPAC, to retarded re-saturation of the infrastructure area, but this is not considered relevant for PA, so that this simplification seems admissible.

As will be seen (Fig. 7) re-saturation beyond the seals occurs far more rapidly, being predominantly driven by compaction rather than shaft inflow. Therefore, it can be concluded that summarizing the materials for this shaft design is a permissible simplification when utilizing the harmonic average of the layers weighted by the thickness of each layer for permeability and using the arithmetic average of the porosities, weighted by the thickness of each layer, since the effect on the overall time for re-saturation of the shaft and infrastructure areas is small.

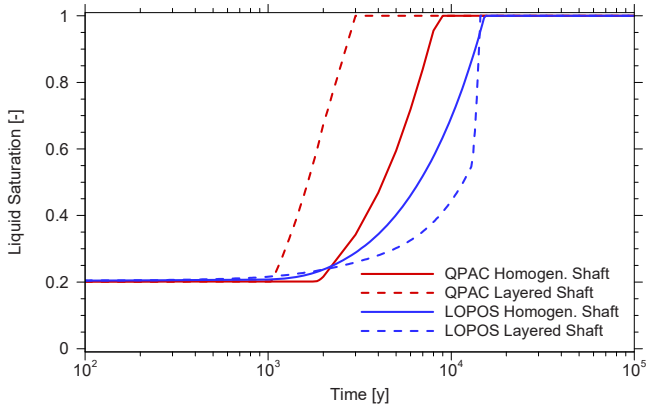

Fig. 5. Saturation of the infrastructure area calculated by LOPOS and QPAC for the homogeneous and the layered shaft case.

3.3. Flow assumptions

In QPAC, all three flow models were applied: Multiphase Flow (MPF), Richards Equation (RE), and Darcy Flow (DF). In LOPOS, calculations are always performed using Darcy's law. However, it is done once with initial complete saturation (which is compared to DF in QPAC and PFLOTRAN) and labelled as LOPOS DF and once with partially saturated compartments. Although Richards equation is not solved, the latter case is denoted as LOPOS RE, as it is compared with the RE calculations with QPAC and PFLOTRAN.

In the case of QPAC, small variations arise due to the employed flow model. These are related to the confinement of air inside the repository when no part of the sealing system is fully saturated. This is due to the treatment of gas as infinitely mobile in the Richards Equation. However, the results remain largely consistent.

3.3.1. Influence of flow assumptions on radionuclide transport

The QPAC results indicate that when assuming DF, the Tracer 1 flow out of the emplacement drift for SNF is initially lower than MPF and RE curves but gradually approaches those curves, which exhibit a very similar trend (Fig. 6, left).

The LOPOS results indicate that the Tracer 1 transport is at first larger when DF is assumed instead of RE, and smaller for later times. The Tracer 1 flow in LOPOS is influenced by compaction (Fig. 6, right). Since the compartment is initially fully saturated, the reduction of pore volume/porosity occurs much more slowly, and squeezing is hindered. In QPAC as well, the reduction in porosity occurs more slowly, but begins earlier. The compaction is then largely completed in less than 100 y, and so has a less significant impact on the Tracer 1 flow, since the tracer is released after 500 years. Therefore, the effect is not visible. Due to the different evolution of porosity, DF between QPAC and LOPOS is not directly comparable. However, LOPOS RE and QPAC RE produce qualitatively similar results. In the beginning the Tracer 1 flow calculated by LOPOS RE is an order of magnitude lower than by QPAC RE, but the results converge at later times. In view of the different numerical concepts of both codes and the fact that LOPOS RE actually does not solve Richard's equation, this can be seen as a fair agreement. QPAC's results suggest that there is no knowledge gain from assuming MPF instead of RE when considering the dissolved radionuclide flows. Since the differences in LOPOS are primarily attributed to the altered saturation and the associated compaction, the LOPOS data will not be further discussed below, and conclusions will be drawn only from the QPAC and PFLOTRAN results.

3.3.2. Influence of flow assumption on saturation

The evolution of the saturation of the emplacement drift for SNF is very similar for the flow models (Fig. 7, left). The delayed saturation in PFLOTRAN RE is discussed in the next section. The difference between RE and MPF is that in the case of MPF in QPAC, the saturation does not reach 1.0 but reaches a maximum of 0.98 due to trapping of the initial air. So after 100,000 years, 2 % air is still present. Taking into account air dissolution (not shown) led to minor alterations in the results, mainly affecting liquid saturation after the shaft reaches full saturation. This reflects the fact that there is minor flow out of the repository, thus gas is trapped, which could eventually become a problem if there was significant corrosion.

3.3.3. Influence of flow assumption on fluid flow

The liquid flow simulated by QPAC is affected by the choice of flow models. When using DF, the liquid flow is initially and at later times higher than liquid flow calculated with MPF and RE (Fig. 7, right). Liquid flow as calculated with DF only falls below the MPF and RE curves between one and 40 years. This difference arises because, during

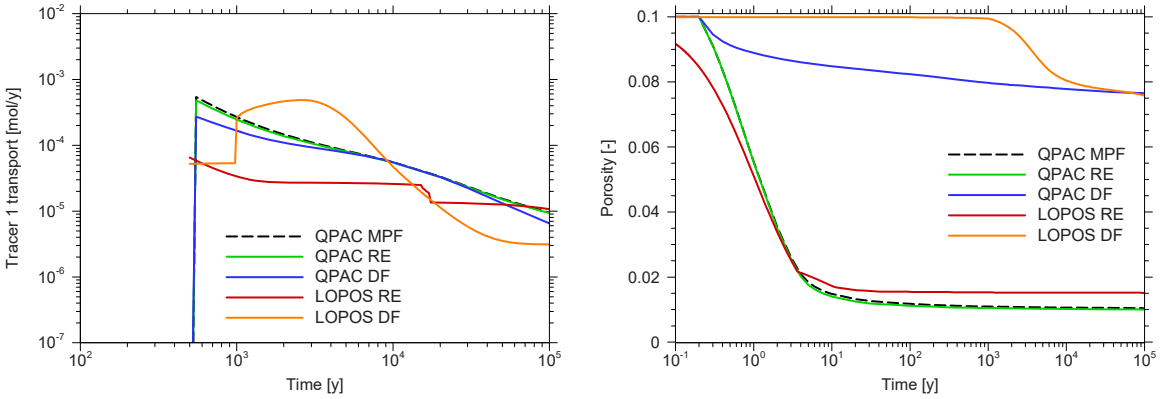

Fig. 6. Comparison of the Tracer 1 flow from and porosity of the emplacement drift for SNF for the various flow models using QPAC and LOPOS.

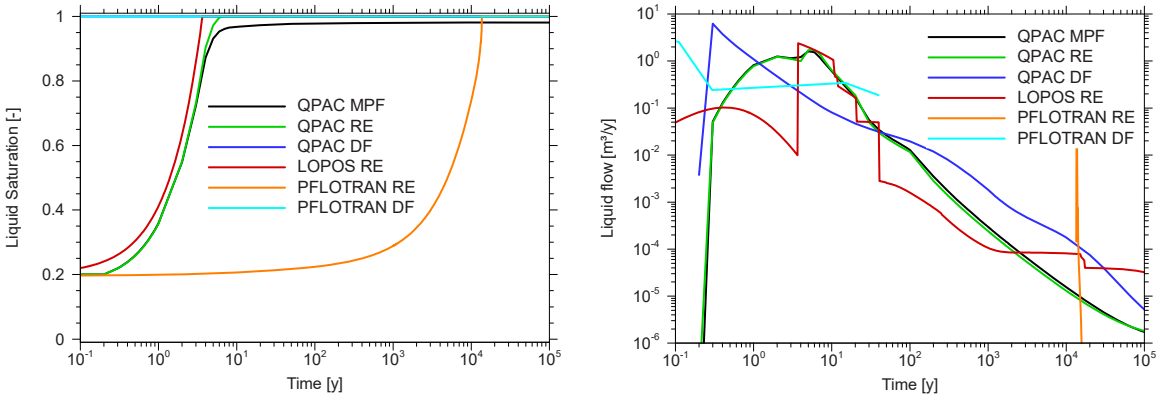

Fig. 7. QPAC, LOPOS and PFLOTRAN results of the liquid saturation (left) and the liquid flow (right) from the emplacement drift for SNF. When the liquid flow in PFLOTRAN turns negative, it is not depicted on the logarithmic scale.

this time period, the emplacement drift reaches full saturation, porosity decreases to 1 %, leading to significant compaction, with squeezing having the most impact. This effect is less pronounced in the case of DF as illustrated in Fig. 6. The liquid flow calculated by LOPOS (RE) follows the same trend compared to that of QPAC (RE). Since saturation in PFLOTRAN takes longer due to neglecting the pore volume decrease, there is liquid flow out of the emplacement drift only after 10,000 years. Flow out of the emplacement drift occurs only for a short period of time, before becoming negative (towards the emplacement drift, not shown on log scale). With DF assumption liquid saturation is initially 1, therefore there is liquid flow out of the drift initially, but the flow turns towards the emplacement drift after 50 years. This change to flow towards the emplacement drifts is in both cases related to how the pressure re-equilibrates within the drifts. The disposal drifts experience a slower increase in pressure than the drift that is connected to them, thus the higher pressure in the drift connecting the disposal drift pushes water into the disposal drift at 50 years. The higher pressures in the drift that connects the disposal drifts is caused by the amount of intact salt adjacent to this drift. Intact salt has higher liquid pressures than the drifts and as a result, having more intact salt adjacent to this drift relative to the disposal drifts causes pressure to increase more quickly.

The liquid flow is very similar when using MPF and RE here, with the only difference being a small amount of trapped gas (2 % saturation) that is slow to migrate in the MPF case. It is therefore concluded that it is permissible to retain the simplified approach of using RE, for the current modelling assumptions.

3.4. Compaction models

All models suggest that salt compaction is a crucial process in the repository. Teams have made different assumptions regarding salt compaction in their models. These assumptions encompass fully-coupled compaction for LOPOS and QPAC, and a stepped permeability change by seven orders of magnitude after 1000 years, for PFLOTRAN.

3.4.1. *Influence of salt compaction on porosity and saturation*

In the models that incorporate compaction (QPAC and LOPOS), compaction leads to a consistent porosity decrease. The porosity evolution curves mirror the compaction assumptions. LOPOS and QPAC exhibit similar curves (Fig. 8, left). This is because the LOPOS compaction model was used to formulate the compaction equations in the task specification, and Quintessa fully integrated these equations into QPAC.

LOPOS and QPAC demonstrate an inverse relationship between liquid saturation and porosity (Fig. 8, left) since porosity decrease leads to a reduced pore volume and less liquid is needed to fill this (Fig. 8, right). PFLOTRAN does not decrease the porosity when representing compaction, therefore more pore volume needs to be saturated and full saturation state is reached later. In the LOPOS and QPAC model porosity decreases to approximately 2 % within the first 100 years, a result of the initial 10 % porosity with 20 % saturation.

3.4.2. *Influence of salt compaction on fluid flow*

LOPOS and QPAC, which calculate porosity reduction resulting from creep closure, show that fluctuations in the rate of salt compaction have a substantial impact on fluid flow within the repository, especially at early times. The models showed that salt compaction was the primary driving force for fluid flow within the repository. This process led to the squeezing of liquid from the waste disposal drifts and into the concrete abutments. LOPOS and QPAC exhibit a similar peak in fluid flow out of

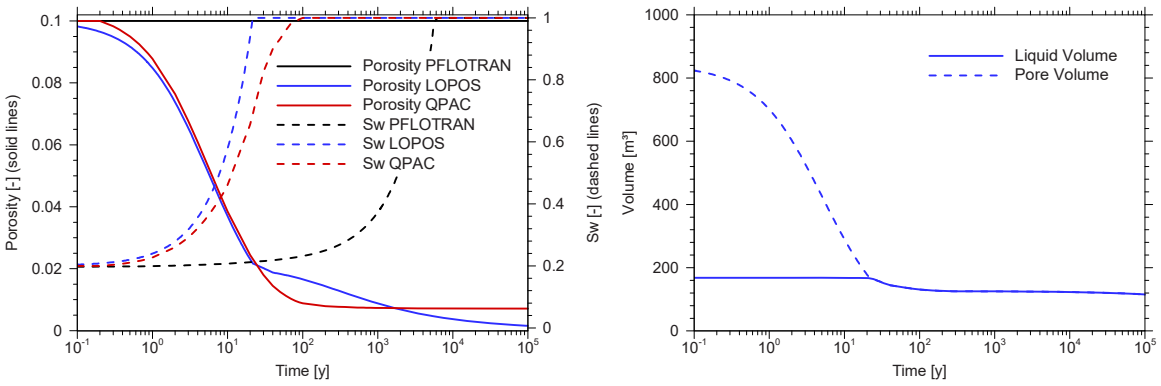

Fig. 8. Porosity and Liquid Saturation of Salt Seal computed with PFLOTRAN, QPAC and LOPOS (left). Associated liquid and pore volume of the Salt seal compartment as computed with LOPOS (right).

the emplacement drift for SNF (shown as LOPOS RE and QPAC RE in Fig. 7, right) after approximately three years and have a very similar trend after 200 years. LOPOS shows this peak after 3 years when this emplacement compartment is fully saturated. After that there is a decrease in fluid flow as calculated with LOPOS. After 10 years, a marked reduction occurs due to the full saturation of the connecting drift. Subsequently, a rapid decline at the 20-year mark is a result of complete saturation in the salt seal. Another decrease in fluid flow is observed after 40 years, attributed to the full saturation of Seal-2 by that time. This is the result of a spontaneous pressure increase when a LOPOS compartment reaches full saturation. In LOPOS a compartment must reach full saturation before liquid squeezing initiates. This is because LOPOS can only simulate single-phase transport. The squeezing of liquid from other compartments and their decreased pore volume, causes the reduction of outflow of liquid from the considered disposal compartment. PFLOTRAN shows a negative fluid flow (not shown on log scale) into the emplacement drift. Liquid only starts flowing out of the emplacement drift calculated with PFLOTRAN at a very late stage. This is because in PFLOTRAN, the saturation process takes longer, and no pore volume reduction or squeezing is considered.

3.4.3. *Influence of salt compaction on radionuclide transport*

Porosity reduction may have limited impact on radionuclide transport out of the emplacement drift for SNF since the main compaction occurs before the SNF waste packages breach, which happens at 500 years. However, squeezing accelerates the radionuclide transport.

Results from QPAC, PFLOTRAN and LOPOS (Fig. 9, left) indicate a beginning of Tracer 1 transport out of the SNF drift immediately following the breach of waste packages at 500 years, which is due to the instant release fraction (IRF) of Tracer 1. This peak is subsequently followed by a decline. This reduction coincides with the decrease in liquid flowrate (Fig. 7, right), diminishing the influence of advection on Tracer 1 transport. All models predominantly give diffusion as the primary transport mechanism and calculate comparable transport of Tracer 1 out of the SNF drift.

In the PFLOTRAN model, liquid flows into the SNF drift after 500 years (due to longer repository resaturation), so that Tracer 1 can only be transported out of the drift through diffusion. Notably, in the PFLOTRAN model, the transport of Tracer 1 via diffusion is quite similar to that of QPAC. The transport of Tracer 3 out of the emplacement drift for HLW (Fig. 9, right) is initially lower in PFLOTRAN. However, after 1000 years, the PFLOTRAN results becomes very similar to that of QPAC. This difference at early times illustrates the impact of squeezing in the QPAC (and LOPOS) model, which isn't present in PFLOTRAN. This difference is likely due to the very different evolution of the PFLOTRAN model where porosities remain unchanged and relatively high, but water saturations remain low. This difference has a large impact on the diffusion process with effective diffusivities being much higher than in the QPAC and LOPOS models during the assessment period, but the effective storage volume for transport is also much larger.

All teams employed the effective diffusion coefficients as outlined in the task specification (LaForce et al.[1]), linking them to porosity. However, due to variations in porosity evolution among the models, it is possible that the models may have different effective diffusion coefficients throughout the simulation.

Even though PFLOTRAN (which is neglecting the porosity reduction and squeezing process) calculates similar tracer transport results

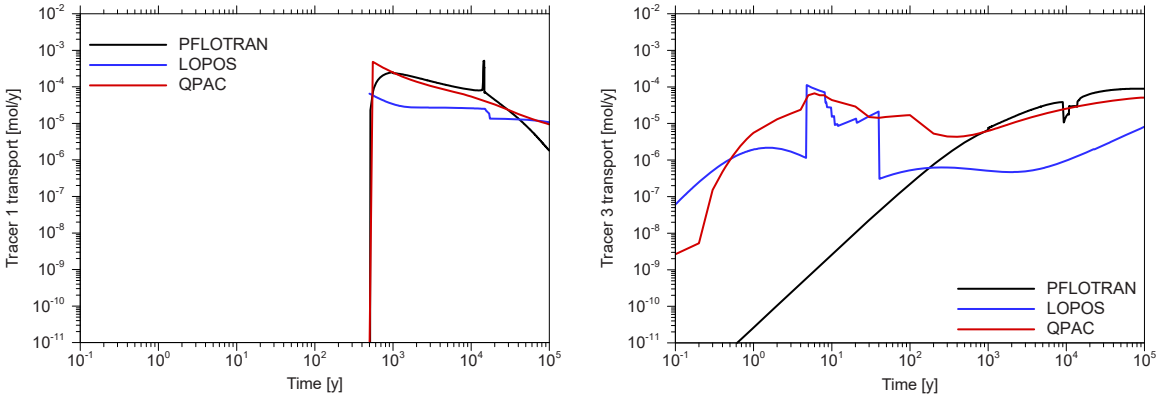

Fig. 9. Flow of Tracer 1 from the emplacement drift for SNF (left) and flow of Tracer 3 (right) from the emplacement drift for HLW as computed with PFLOTRAN, LOPOS and QPAC. Jumps in LOPOS results are due to stylized modelling of RN transport. The peak around 1.5E4 years in PFLOTRAN results (left) is associated with the drift becoming 100 % liquid saturated.

compared to LOPOS and QPAC, it is important to know when the permeability needs to be reduced and to what extent to capture the reduction in advective flow of liquid in the repository in PFLOTRAN. Additionally, the squeezing out of liquid is an important process, which could cause advection in the repository and thereby alter the flow regime in the repository. The differences in liquid flow and tracer transport reflect the significance of integrating a high-fidelity salt compaction model into salt PA models for the study of repository performance.

In our study, waste package failure was set to a pessimistically early point in time, in order to cause relevant radionuclide transport. In a real case, compaction is likely to have come to an end before any release from the canisters takes place, and transport will be diffusion-dominated.

3.5. Initial conditions

Initial conditions are challenging to determine for generic repositories, but they have a significant impact on the system's behaviour. The initial saturation is an important factor in shaping the evolution of the repository. The amount of liquid accelerates the compaction process, more quickly reaching complete saturation in the compacted pore space. This, in turn, triggers the squeezing phase of fluid transport earlier, impacting the transport of radionuclides and tracers if any are present at that time. On the other hand, an initial saturation of 20 % leads to supporting pressure as soon as the pore volume is reduced to match this initial amount of liquid, so that the rate of pore volume reduction slows down. The high initial saturation in the shaft directly provides more liquid available to flow into the repository. The high initial saturation was chosen because PFLOTRAN was numerically unable to calculate with residual saturation. When considering an initially residual-saturated shaft (3 %), LOPOS calculates a higher liquid inflow rate prior to shaft failure, which can result in radionuclides and tracer being mobilized earlier. In QPAC, it's different because the shaft must be almost completely saturated before liquid transport to the repository is calculated. The difference here is that complete saturation is reached faster with an initial saturation of 35 %, allowing the solution to reach the waste earlier. However, this deviation has only minor impacts on the overall system behaviour.

Regarding the parameterization of convergence, it is essential in the chosen approach to carefully select the initial convergence rate, as it has the most significant influence on the compaction's progression. A variation was conducted which showed that with slower compaction and residual saturation as initial condition the transport of radionuclides is changed, due to compaction influencing fluid movement. It has been observed that both convergence and diffusion have the most substantial impact on model outcomes, underscoring the critical importance of initializing these parameters thoughtfully.

It is concluded that it is important to conduct a careful analysis and modelling to understand the impact of these parameters on the safety of the repository and to take appropriate measures to minimize uncertainties for specific assessments. For example, for "expected evolution scenarios", where waste package failure would be expected to occur after salt convergence and resaturation of shaft and infrastructure features, it may be sufficient to simulate only a post-compaction steady state porosity and fluid system. Whereas, for early release scenarios, a more detailed model of the system evolution from the state at repository closure may be required.

3.6. Geosphere inflow

If we assume that liquid can infiltrate from the surrounding intact salt despite the low permeability of 10^{-22} m^2, then it's evident that the presence of liquid inflow does have some influence on the liquid disposition in the repository.

In the PFLOTRAN model, the key driving forces for resaturation are inflow from the geosphere, occurring at a rate in the order of 10^{-5} m^3 / yr and inflow from the shaft, which occurs after 1000 years. The flow rate entering the repository by the shaft is depicted in Fig. 10 (left). In the PFLOTRAN model, there are two key driving forces for resaturation, in early time (<1000 years) the only inflow is from the geosphere, occurring at a rate in the order of 10–5 m^3/yr and then resaturation is driven by inflow from the shaft, which occurs after 1000 years. It is important to note that the process of resaturation through these two mechanisms is slow in PFLOTRAN. This limits the liquid present in the repository, which serves as a transport medium for the radionuclides/tracers. For comparison, the total amount of liquid that is intruding the repository from the shaft as calculated with PFLOTRAN, LOPOS and QPAC is depicted in Fig. 10 (right). This exceeds the 10^{-5} m^3 /y geosphere inflow in PFLOTRAN (in total 1 m^3), by multiple orders of magnitude.

QPAC calculated the base case without any inflow from the geosphere, but as a variation, accounted for this inflow, but this doesn't fundamentally alter the system's evolution. The QPAC results suggest that Seal 1 has resaturated, as it is no longer deprived of a liquid source. This has led to a slight increase in discharge past Seal 2 but a decrease in discharge past Seal 1. However, the overall differences are relatively small.

4. Conclusions

Clearly, simplifications within PA models are essential, but they should be made carefully to maintain the integrity of the model's meaningfulness. Our study has yielded several important insights for the specific disposal concept that is considered. First, we have found that there are no restrictions resulting from the variations in geometry that

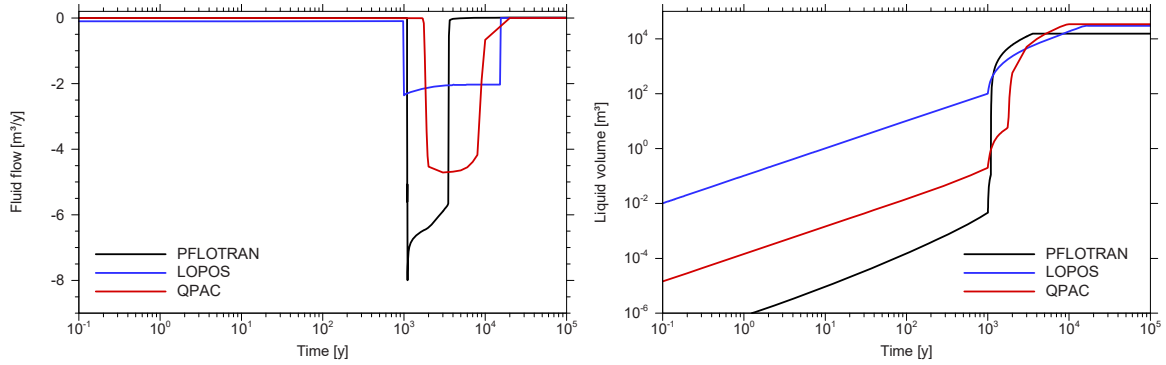

Fig. 10. Fluid flow from the shaft (left) (negative values indicate flow towards the repository, whereas positive flow indicates flow towards the overburden; the PFLOTRAN flow reaches a slightly positive value of 0.01 at the end (LOPOS and QPAC reach exactly 0), and the total liquid volume (right) entering the repository from the shaft.

were analysed. Additionally, it is considered a conservative approach to consolidate the layered shaft materials into a homogeneous shaft. This simplification is deemed acceptable for the chosen parameterization and current modelled processes. Furthermore, when comparing different flow models, we observed minor deviations in liquid saturation and flow. These minor differences do not permit the conclusion that two-phase processes are negligible, especially if gas sources in the repository are considered in future calculations. It can only be inferred that, for this parameterization of the processes and this modelling task, the application of the Richards' equation is sufficient. These specific simplifications are expected to be applicable to the modelling of similar repository designs. However, other aspects of alternative repository designs will need to be analysed separately to understand the further simplifications that may be allowable.

The permissible simplifications that were made resulted in accelerated computation times, which is crucial in performance assessment, as a large number of calculations is required for the associated sensitivity analyses. Significant disparities in both liquid flow and tracer transport, mainly in the early phase, were observed between, on the one side, QPAC and LOPOS, which take into account salt compaction, and, on the other side, PFLOTRAN, which does not. With unsaturated starting conditions, LOPOS and QPAC reach full saturation after a few years, while PFLOTRAN needs more than 10,000 years. This underscores the critical importance of a high-fidelity salt compaction model in the context of PA modelling in salt formations. There remains a need for further research on the level of detail required for modelling compaction in this context. The salt compaction approach implemented in QPAC and LOPOS (see Section 2.3.4) is well-established. Nevertheless, due to the current state of knowledge, it is essential to perform calculations that take into account the gas phase, and a revision of this approach is necessary, as the inclusion of trapped air has an impact on the pressure development and radionuclide transport.

A key insight from our research underscores the significance of exercising caution when defining and implementing models. It is noteworthy that various considered processes can yield similar outcomes. For instance, in the case of PFLOTRAN, not including the reduction in pore volume due to convergence, leads to an extended saturation process. However, when it comes to the transport of tracers and radionuclides, the behaviour remains fairly consistent with LOPOS and QPAC because diffusion serves as the primary transport mechanism and additionally the PFLOTRAN model, was the only implementation that included inflow from the geosphere. Initial conditions have a large impact on the results of the calculations. It is important to consider what is being defined in order to then interpret the results, and hence suggests that the use of multiple approaches and progressive increases in complexity is extremely important in producing models that are well-understood and defensible against the required modelling endpoints. Clearly, the initially high saturation and the fast compaction have a significant influence on the model examined. These two effects and diffusion determine the system behaviour and can look different with less generic assumptions.

With various simplifications and abstractions, QPAC, PFLOTRAN, and LOPOS yield different, yet fairly similar results. The relative importance of the differences depends on the criteria used to compare the models. For example, if initial waste package defect scenarios are to be considered, then a model that is capable of simulating re-saturation and transport in partially saturated conditions is required, but for later failures a model that can simulate only diffusive transport in converged steady-state porosity conditions may be sufficient. The interpretation of the results concerning what is considered in the modelling as input is crucial. Detailed uncertainty and sensitivity analysis can be a valuable tool for determining the significance of parameters and conditions and for identifying further admissible simplifications. Ultimately, the applied computational tools complement each other well in their capabilities and align on the most significant conclusions, particularly regarding the distance the tracers and radionuclides reach from the disposal drifts.

CRediT authorship contribution statement

Jens Wolf: Supervision. **Tanja Frank:** Writing – original draft, Investigation. **Steven Benbow:** Writing – review & editing, Investigation. **Dirk-Alexander Becker:** Writing – review & editing, Investigation. **Richard Jayne:** Writing – review & editing, Investigation. **Alexander Bond:** Writing – review & editing, Project administration, Investigation. **Tara LaForce:** Writing – review & editing, Project administration, Investigation.

Declaration of Competing Interest

The authors declare that they have no known competing financial interests or personal relationships that could have appeared to influence the work reported in this paper.

Data availability

Data will be made available on request.

Acknowledgements

DECOVALEX is an international research project comprising participants from industry, government and academia, focusing on development of understanding, models and codes in complex coupled problems in sub-surface geological and engineering applications; DECOVALEX-2023 is the current phase of the project. The authors appreciate and thank the DECOVALEX-2023 Funding Organisations Andra, BASE, BGE, BGR, BMUV, CAS, CNSC, COVRA, US DOE, ENRESA, ENSI, JAEA, KAERI, NWMO, NWS, SÚRAO, SSM and Taipower for their financial and technical support of the work described in this paper. The statements made in the paper are, however, solely those of the authors and do not necessarily reflect those of the Funding Organisations.

This article has been authored by an employee of National Technology & Engineering Solutions of Sandia, LLC under Contract no. DE-NA0003525 with the U.S. Department of Energy (DOE). The employee owns all right, title and interest in and to the article and is solely responsible for its contents. The United States Government retains and the publisher, by accepting the article for publication, acknowledges that the United States Government retains a non-exclusive, paid-up, irrevocable, world-wide license to publish or reproduce the published form of this article or allow others to do so, for United States Government purposes. The DOE will provide public access to these results of federally sponsored research in accordance with the DOE Public Access Plan https://www.energy.gov/downloads/doe-public-access-plan. This paper describes objective technical results and analysis. Any subjective views or opinions that might be expressed in the paper do not necessarily represent the views of the U.S. Department of Energy or the United States Government.

References

1.. LaForce T, Jayne R, Leone R, Mariner P, et al. DECOVALEX-2023-Task F-Specification Revision 10; 2023.
2.. Bollingerfehr W, Bertrams N, Buhmann D, Eickemeier R, et al. Concept Developments for A Generic Repository for Heat-generating Waste in Bedded Salt Formations in Germany, Project KOSINA. Synthesis Report. BGE TEC. Peine (BGE TEC 2018-13); 2018.
3.. Bertrams Niklas, Bollingerfehr Wilhelm, Eickemeier Ralf, Fahland, Sandra. RESUS - Grundlagen zur Bewertung eines Endlagersystems in steil lagernden Salzformationen. Gesellschaft für Anlagen- und Reaktorsicherheit. Köln, Garching b. München, Berlin, Braunschweig (GRS, GRS-569); 2020.
4.. Bohlingerfehr W, Filbert W, Dörr S, Herold P, et al. Endlagerauslegung und -optimierung. Bericht zum Arbeitspaket 6, Vorläufige Sicherheitsanalyse für den Standort Gorleben. Köln (GRS-281); 2012.

5.. Meleshyn Artur, Noseck Ulrich. Radionuclide Inventory of Vitrified Waste after Spent Nuclear Fuel Reprocessing at La Hague. Basic Issues and Current State in Germany. Köln, Berlin (GRS-294); 2012.
6.. Blanco-Martin L, Rutqvist J, Battistelli A, Birkholzer JT. Coupled processes modeling in rock salt and crushed salt including halite solubility constraints: application to disposal of heat-generating nuclear waste. *Transp Porous Media*. 2018;124 [Hg. v].
7.. Rübel André Peter, Buhmann Dieter, Kindlein Jonathan, Lauke Thomas. Performance Assessment of Sealing Systems. Conceptual and Integrated Modelling of Plugs and Seals. Köln (GRS-415); 2016.
8.. Ecay L, Grégoire D, Pijaudier-Cabot G. On the prediction of permeability and relative permeability from pore size distributions. *Cem Concr Res*. 2020;133 [Hg. v].
9.. Osselin F, Fabbri A, Fen-Chong T, Pereira J, Lassin A, Dangla P. Experimental investigation of the influence of supercritical state on the relative permeability of vosges sandstone. *C R Mécanique*. 2015 [Hg. v. 343].
10.. Hammond GE, Lichtner PC, Mills RT. Evaluating the performance of parallel subsurface simulators: an illustrative example with PFLOTRAN. *Water Resour Res*. 2014;50 [Hg. v].
11.. Quintessa. QPAC: Quintessa's General-Purpose Modelling Software. (QRS QPAC-11); 2013. Available under ⟨http://www.quintessa.org/qpac-overview-report.pdf⟩.
12.. Hirsekorn Rolf-Peter, Boese Brigitte, Buhmann Dieter, Hirsekorn R-P. LOPOS. Programm zur Berechnung der Schadstofffreisetzung aus netzwerkartigen Grubengebäuden. Gesellschaft für Anlagen- und Reaktorsicherheit. Köln (GRS-157); 1999.
13.. Reiche T. RepoTrend - das Programmpaket zur integrierten Langzeitsicherheitsanalyse von Endlagersystemen. Braunschweig (GRS-413); 2016.
14.. Frieling G., Kock I. Modellkonzepte, Prozesse und Rechenfälle für das Vorhaben ZIESEL. Synthesebericht Teil 2/2 Zweiphasenfluss in einem salinaren Endlager am Beispiel des ERAM. Köln (GRS-397); 2016. Available under ⟨https://www.grs.de/sites/default/files/publications/grs-397_0.pdf⟩.
15.. Larue J, Baltes B, Fischer H, Frieling G, et al. Radiologische Konsequenzenanalyse. Bericht zum Arbeitspaket 10; vorläufige Sicherheitsanalyse für den Standort Gorleben. Garching (GRS-289); 2013.
16.. Bond AE, Thatcher KE, Norris S. Multi-scale gas transport modelling for the EC FORGE project. *Mineral Mag*. 2015;79(6):1251–1263 [Hg. v].
17.. Noseck Ulrich, Brewitz W, Becker D-A, Buhmann D, et al. Wissenschaftliche Grundlagen zum Nachweis der Langzeitsicherheit von Endlagern. Gesellschaft für Anlagen- und Reaktorsicherheit. Köln, Garching b. München, Berlin, Braunschweig (GRS-204); 2005.
18.. Storck Richard, Buhmann D, Hirsekorn R-P, Kühle T, Lührmann L. Das Programmpaket EMOS zur Analyse der Langzeitsicherheit eines Endlagers für radioaktive Abfälle. Version 5. Gesellschaft für Anlagen- und Reaktorsicherheit. Köln, Garching b. München, Berlin, Braunschweig, Braunschweig (GRS 122); 1996.
19.. Becker D-A, Buhmann D, Mönig J, Noseck U, Rübel A, Spießl S. Endlager Morsleben. Sicherheitsanalyse für das verfüllte und verschlossene Endlager mit dem Programmpaket EMOS. Bundesamt für Strahlenschutz, Verfahrensunterlage P278; 2009. Available under ⟨https://archiv.bge.de/archiv/www.endlager-morsleben.de/SharedDocs/Downloads/Morsleben/DE/planfeststellungsverfahren/lfdnr106-278-00-v01-p278b1dd.pdf?_blob=publicationFile&v=1⟩.